



Beam Deflections and Stresses during Lifting

R.H. Plaut¹, C.D. Moen², R. Cojocaru³

Abstract

The behavior of beams during lifting is analyzed. The beams are circularly curved (horizontally), doubly symmetric, prismatic, and linearly elastic, and are suspended at two symmetric locations. The two cables lifting the beams may be vertical or inclined symmetrically. Numerical results are presented for steel I-beams. Weak-axis and strong-axis deflections, roll angle and cross-sectional twist, internal forces, bending and twisting moments, and longitudinal stresses are calculated using newly derived analytical solutions. Lifting locations along the beam that minimize displacements and stresses are identified.

1. Introduction

When a horizontally curved beam is lifted by two cables, it tends to roll (rotate) about an axis above the beam. This causes weak-axis bending and cross-sectional twist to occur. Excessive roll and twist may cause difficulties when the beam is put into place, e.g., on permanent or temporary bridge supports. The objectives of the present study are to obtain analytical solutions for a basic class of beams and to determine the effects of various parameters, such as the locations of the lift points. For suspended beams that are intentionally curved, or are meant to be straight but have an imperfection in shape, the displacements and stresses are of concern, and lateral buckling is typically not an issue (Petruzzi 2010; Plaut and Moen 2011).

In the analysis, the beams are circularly curved (horizontally), the curvature is small, and the cross-sectional dimensions are small compared to the radius of curvature. The cross section is uniform and doubly symmetric, and its center of gravity coincides with its shear center. The material behavior is linearly elastic and the displacements are small. The beam is subjected to its self-weight and to the two supporting cable forces, which are symmetric with respect to midspan.

Investigations on the lifting of straight or curved beams include Mast (1989), Dux and Kitipornchai (1990), and Stratford and Burgoyne (2000). Additional references are listed in Plaut and Moen (2011). A recent research project at the University of Texas at Austin studied the behavior of curved steel I-beams during lifting with vertical cables (e.g., Farris 2008; Schuh

¹ D. H. Pletta Professor of Engineering (Emeritus), Virginia Tech, <rplaut@vt.edu>

² Assistant Professor, Virginia Tech, <cmoen@vt.edu>

³ Graduate Research Assistant, Virginia Tech, <cojocaru@vt.edu>

2008; Petruzzi 2010; Stith 2010). Results of some tests were presented, and the analysis was mainly conducted using the finite element software ANSYS. A software program, UT Lift, was developed, plus another program, UT Bridge, that involves construction of bridges.

The present investigation complements the UT research. The focus is not only on steel I-beams, and the supporting cables may be inclined. Instead of applying the finite element method, the results are obtained from new analytical equations (Plaut and Moen 2011). However, this study is more restricted in some aspects, since it does not include nonprismatic beams, nonsymmetric lift points, or the effect of attached cross frames.

2. Formulation

The beam is depicted in Fig. 1. A perspective with inclined cables is shown in Fig. 1(a), a top view in Figs. 1(b) and 1(c), a side view (from the center of curvature) in Fig. 1(d), and another perspective in Fig. 1(e). The unstrained beam has radius of curvature R , length L , cross-sectional area A , modulus of elasticity E , shear modulus G , torsional constant J , warping constant C_w , and self-weight q per unit length.

The subtended angle of the beam is 2α , and the cylindrical coordinate θ is zero at midspan. The connection points D and K of the two cables are located at the lift points $\theta = -\gamma$ and γ , respectively, at a distance a from the near end of the beam, and at a height H above the shear center and parallel to the y axis (i.e., the weak axis). The line passing through D and K , which is dashed in Fig. 1(e), is called the roll axis (or axis of rotation). The inclination angle of the cables from the vertical is ψ toward midspan, and the offset of the center of the beam from the chord through the ends is denoted δ .

Fig. 1(a) shows the principal axes y and z of the cross section, and the longitudinal x axis, which is tangential to the curved axis of the member through the shear center. The origin is at midspan, so that $x = R\theta$. The longitudinal deflection is U , the strong-axis deflection is V , the weak-axis deflection is W (positive if radially outward), and the angle of twist is ϕ . The moments of inertia for strong-axis and weak-axis bending, respectively, are I_z and I_y .

The center of gravity of the unstrained beam lies along the central ray $\theta = 0$ and at a radial distance (eccentricity) e from the roll axis, as shown in Fig. 1(c). If the center of gravity of the whole beam does not lie in the vertical plane that includes the roll axis, then the beam exhibits a rotation about the roll axis, as shown in Fig. 1(e), until its center of gravity lies in that vertical plane. If the beam were rigid, the roll angle would be $\beta_{\text{rigid}} = \text{Arctan}(e/H)$ (Schuh 2008). The deformation causes the actual roll angle β to be different. The total rotation of the plane of the cross section at location θ is $\beta \cos\theta - \phi$, and it is assumed that V , W , and ϕ are zero at the lift points (so that the total rotation there is $\beta \cos\gamma$). The equation for β , along with analytical equations that furnish the internal forces and moments, deflections, twist, and stresses, are given in Plaut and Moen (2011).

The roll angle β is usually zero when a/L is approximately 0.21 (Schuh 2008; Plaut and Moen 2011). For smaller values of a/L , β is positive, and for larger values of a/L , β is negative. As a/L decreases or increases from 0.21, the magnitude of the roll angle increases.

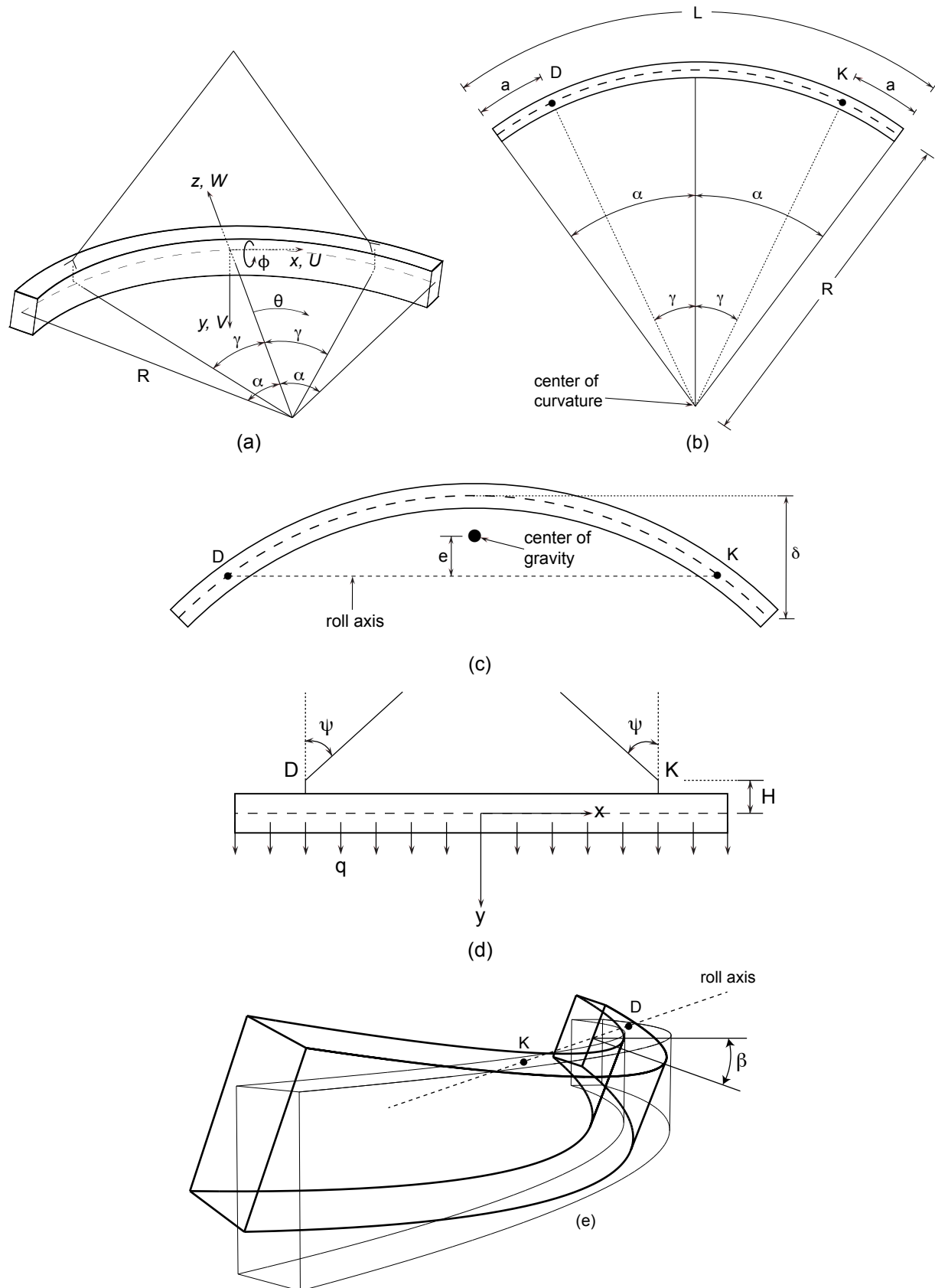


Figure 1: Geometry of beam, (a) perspective, (b) top view, (c) top view, (d) side view, (e) rotation about roll axis

3. Example

Three steel I-beams, similar to ones in Schuh (2008), are considered. The beams have $\delta/L = 0.01$, $L = 90$ ft, $R = 1,125$ ft, web depth $h_w = 69$ in., web thickness $t_w = 0.75$ in., flange thickness $t_f = 1.5$ in., $H = 66$ in., $E = 29,000$ ksi, Poisson's ratio = 0.3, and specific weight = 490 lb/ft³. The cables are vertical ($\psi = 0$). Three flange widths, $b_f = 12$ in., 18 in., and 24 in., are considered, and the corresponding values of A , q , I_y , I_z , J , and C_w are listed in Table 1. The effect of the normalized overhang length is examined for the range $0.1 \leq a/L \leq 0.4$.

Table 1: Properties of steel I-beams

b_f (in.)	A (in. ²)	q (kip/ft)	I_y (in. ⁴)	I_z (in. ⁴)	J (in. ⁴)	C_w (in. ⁶)
12	87.75	0.299	434	65,300	36.7	0.537×10^6
18	105.75	0.360	1,460	87,600	50.2	1.812×10^6
24	123.75	0.421	3,458	110,000	63.7	4.294×10^6

Fig. 2 shows how the roll angle varies with a/L . For small overhang lengths, the roll angle β is positive and the cross section tilts so that its top edge moves outward (away from the center of curvature), as shown in Fig. 1(e). For large overhang lengths, it tilts in the opposite direction. The magnitude of the roll angle tends to decrease slightly as the flange width increases from 12 in. to 24 in.

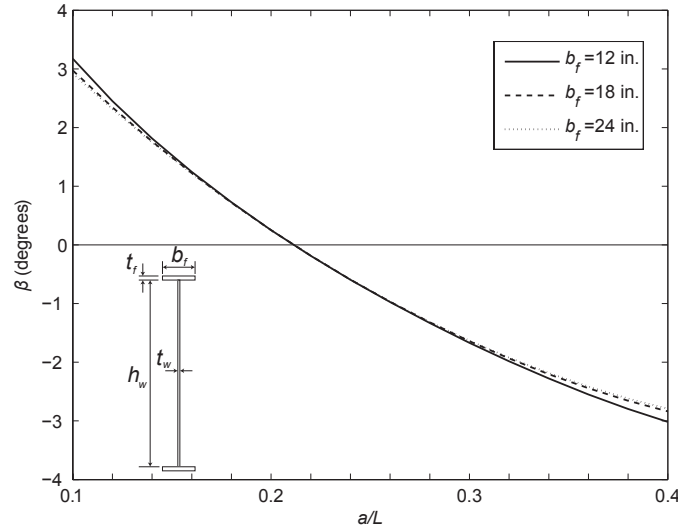


Figure 2: Roll angle versus normalized overhang length a/L

The twist ϕ at midspan is plotted in Fig. 3. It is positive for an intermediate range of the overhang length, and negative otherwise. Fig. 4 depicts how the overhang length affects the twist at the end of the beam ($x = L/2$). For a given value of a/L , as the flange width increases, the magnitudes of the midspan and end twist usually decrease.

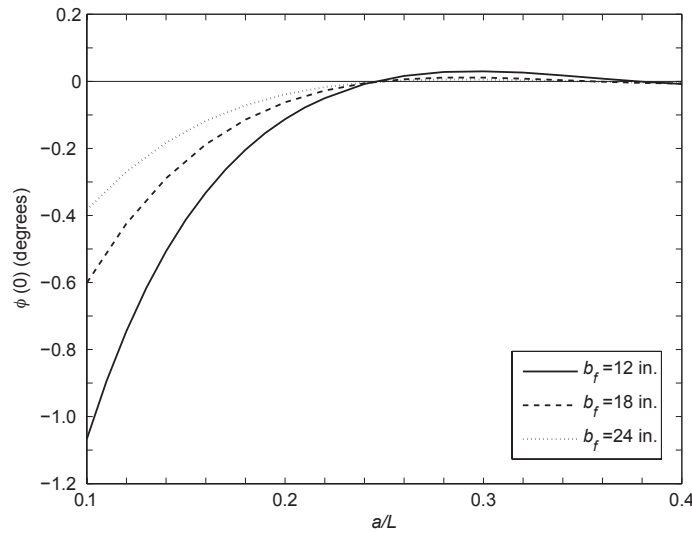


Figure 3: Twist at midspan versus a/L

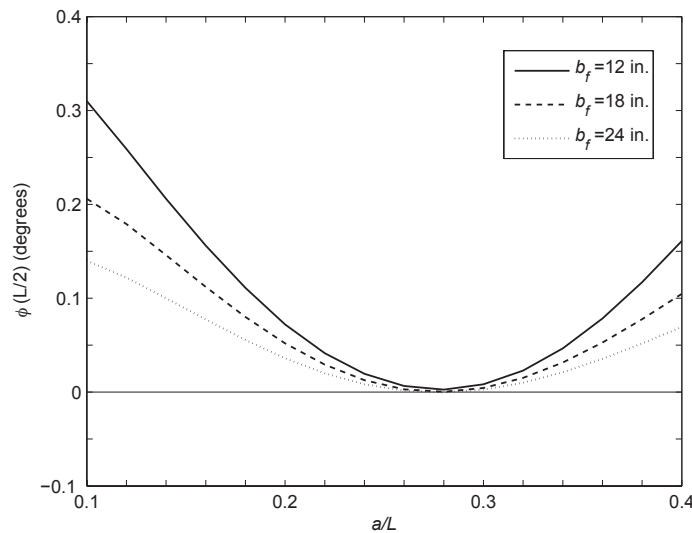


Figure 4: Twist at end versus a/L

It has been recommended that the magnitude of the total rotation, $|\beta \cos\theta - \phi|$, be less than 1.5° (Farris 2008). The overhang length is critical with regard to this criterion. For the three flange widths considered, the criterion is satisfied at midspan if $0.17 < a/L < 0.29$, and at the end of the beam if $0.14 < a/L < 0.29$.

In Fig. 5, the weak-axis deflection W at midspan is plotted versus a/L . The roll angle is zero when $a/L = 0.211$, and this deflection $W(0)$ becomes slightly negative for a small range around $a/L = 0.22$. As the flange width increases, the midspan deflection tends to decrease.

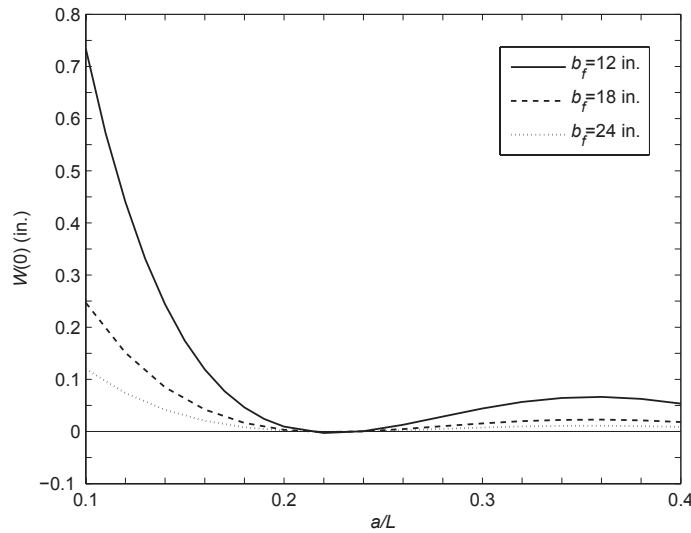


Figure 5: Weak-axis deflection at midspan versus a/L

With regard to possible buckling of the flange due to compression, it is important to know the magnitude of the longitudinal (normal) stress acting on the cross section. The maximum value occurs at midspan, and in general is a combination of stresses due to axial load, weak-axis bending, strong-axis bending, and warping (Seaburg and Carter 1997; Stith 2010). The first of these stresses is zero here because the cables are vertical, i.e., $\psi = 0$. Summing the values of the maximum magnitudes of each of the other stresses at the tips of the flanges, one can write an upper bound as $\sigma_n = |\sigma_{by}| + |\sigma_{bz}| + |\sigma_w|$, where the stress contributions at a tip at midspan are σ_{by} due to weak-axis bending, σ_{bz} due to strong-axis bending, and σ_w due to warping normal stress.

The longitudinal stress σ_{by} due to weak-axis bending is shown in Fig. 6 for the three steel I-beams. It is highest for $b_f = 12$ in. and lowest for $b_f = 24$ in. For all three cases, $\sigma_{by} = 0$ at $a/L = 0.21$ and 0.25 , and σ_{by} is very small if the lift points lie between those locations.

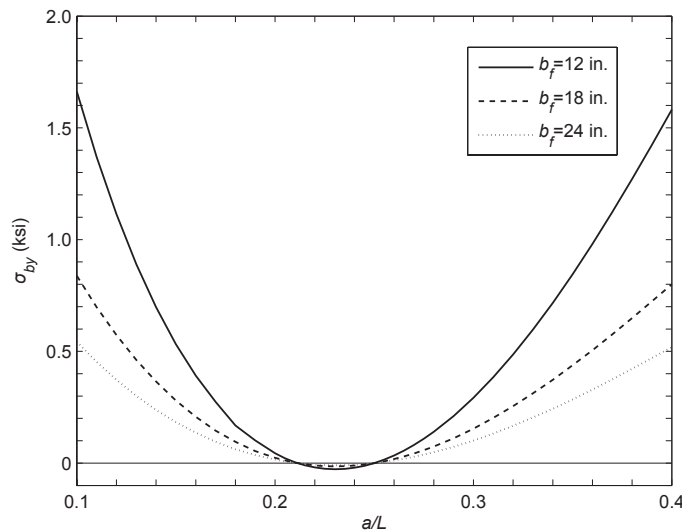


Figure 6: Longitudinal stress at midspan tip due to weak-axis bending versus a/L

Fig. 7 depicts the longitudinal stress σ_{bz} due to strong-axis bending. This stress is zero at $a/L = 0.25$. The highest magnitude occurs for $b_f = 12$ in., the case with the highest ratio A / I_z .

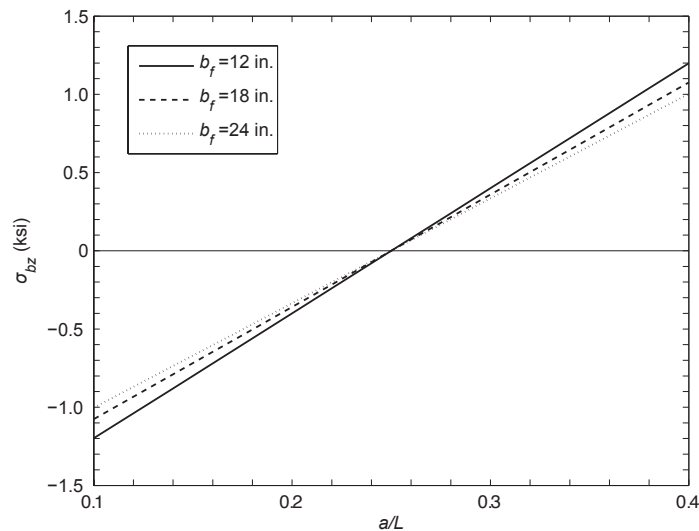


Figure 7: Longitudinal stress at midspan tip due to strong-axis bending versus a/L

In Fig. 8, the midspan stress σ_w due to warping normal stress is plotted. It is zero at $a/L = 0.25$ for the three cases, and again at $a/L = 0.40, 0.37,$ and $0.36,$ respectively, for $b_f = 12, 18,$ and 24 in. In comparing Figs. 6-8, the magnitude of σ_w is larger than the magnitudes of σ_{by} and σ_{bz} for all three cases if a/L is small.

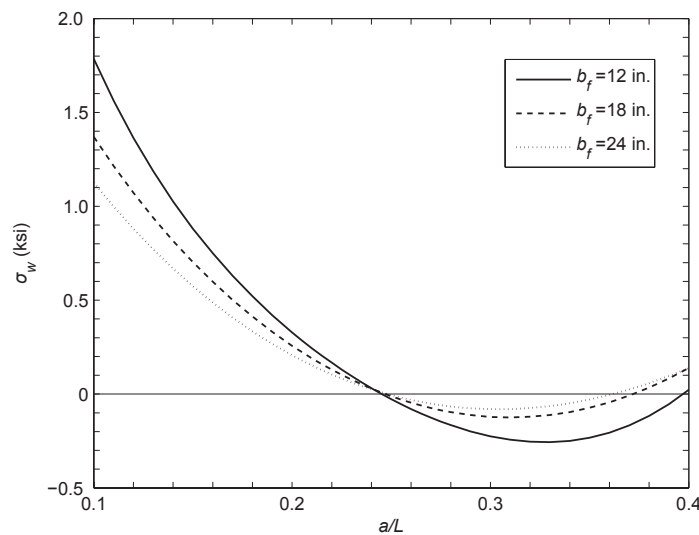


Figure 8: Longitudinal stress at midspan tip due to warping versus a/L

Finally, the sum σ_n of the magnitudes of these three normal stresses is depicted in Fig. 9. It is zero at $a/L = 0.25$, and elsewhere is highest for $b_f = 12$ in. In the range shown, and for these three steel I-beams, the longitudinal stresses are not very large. Similar magnitudes were found in tests reported in Schuh (2008).

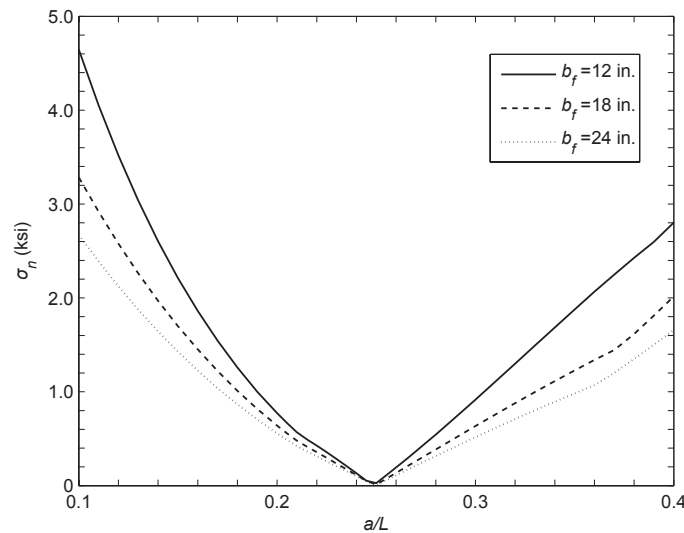


Figure 9: Upper bound on magnitude of longitudinal stress at midspan versus a/L

4. Concluding Remarks

The locations of the lift points are most important. If the distance between each lift point and the near end of the beam is not approximately one-fifth of the beam's length, the beam may rotate significantly and exhibit undesirably large displacements and stresses. It is also important that the torsional constant and the weak-axis moment of inertia not be too small, so that the weak-axis deflection and cross-sectional twist are not too large.

Lateral buckling is possible if the beam is perfectly straight, but even then it will not occur for reasonably designed beams and lift points (i.e., if the bending stiffnesses and torsional stiffness are not extremely small, and the beam is not lifted near its ends). The governing equations for lateral buckling are presented in Plaut and Moen (2011). For the steel I-beams considered here, the corresponding 90-ft-long straight beam would have a critical specific weight that is larger than the specific weight of steel by factors 2.2, 4.4, and 7.4, respectively, if $b_f = 12, 18,$ and 24 in. and if the lift points are at the ends ($a = 0$). The factors are larger if the lift points are not at the ends ($a > 0$).

References

- Dux, P. F., and Kitipornchai, S. (1990). "Stability of I-beams under self-weight lifting." *J. Struct. Eng.*, 116(7), 1877-1891.
- Farris, J. F. (2008). *Behavior of Horizontally Curved Steel I-girders During Construction*, Master's Thesis, University of Texas at Austin, Austin, Texas.
- Mast, R. F. (1989). "Lateral stability of long prestressed concrete beams, Part 1." *PCI J.*, 34(1), 34-53.
- Petruzzi, B. J. (2010). *Stabilizing Techniques for Curved Steel I-girders During Construction*, Master's Thesis, University of Texas at Austin, Austin, Texas.
- Plaut, R. H., and Moen, C. D. (2011). "Analysis of elastic, doubly symmetric, horizontally curved beams during lifting. I: theory." *J. Struct. Eng.*, under review.
- Schuh, A. C. (2008). *Behavior of Horizontally Curved Steel I-girders During Lifting*, Master's Thesis, University of Texas at Austin, Austin, Texas.
- Seaburg, P. A., and Carter, C. J. (1997). *Torsional Analysis of Structural Steel Members*, Steel Design Guide Series 9, American Institute of Steel Construction, Chicago, Illinois.

- Stith, J. C. (2010). *Predicting the Behavior of Horizontally Curved I-girders During Construction*, PhD thesis, University of Texas at Austin, Austin, Texas.
- Stratford, T. J., and Burgoyne, C. J. (2000). "The toppling of hanging beams." *Int. J. Solids Struct.*, 27(26), 3569-3589.